PCIM'90 Conference, Munich, June 25–28, 1990

ANALYTICALLY CLOSED OPTIMIZATION OF THE MODULATION METHOD OF A PWM RECTIFIER SYSTEM WITH HIGH PULSE RATE

JOHANN W. KOLAR, HANS ERTL, FRANZ C. ZACH
Technical University Vienna, Power Electronics Section,
Gußhausstraße 27, Vienna, AUSTRIA

Phone: (int)43 222 58801-3886 Fax: (int)43 222 5052666

Keywords: PWM Converter System, Pulse Pattern Optimization, Harmonic Power Loss

Abstract

By application of the space vector calculus the optimization of the control method of a voltage DC link PWM converter system with high pulse rate can be performed analytically simple without the necessity of using a digital computer. The quality functional is defined by the rms value of the output current harmonics. The optimizing calculation can be performed locally (related to a pulse period and resulting in the determination of a modulation function) or in a global manner (for the parameters of a given modulation function). It is shown that local and global optimization lead to the same results.

As further result there follow modulation functions which make possible a substantial reduction of the harmonic power loss especially in the upper modulation range when compared to the known control functions. The resulting harmonic power losses can be given directly in the form of simple mathematical expressions in dependency of pulse frequency and modulation depth.

Based on the duality relations existing between voltage DC link and current DC link PWM converters furthermore a simple transfer of the results to current DC link PWM converter systems is possible.

1 Introduction

Due to the broad industrial application of converter fed induction motor drives the determination of optimal control methods constitutes an important part of the theory of the stationary operating behavior of PWM converter systems. As optimization criteria one can use, e.g., the maximum appearing current amplitude, or the rms value of the current harmonics generated, or the elimination of certain harmonics. As side condition of the optimization the output voltage fundamental to be generated by the converter system is given.

The determination of the optimal switching instants of the power electronic devices can be performed in a region of lower pulse rates (i.e., for higher power systems) on a digital computer via classical switching

The authors are very much indebted to the Austrian Fonds zur Förderung der wissenschaftlichen Forschung which supports the work of the Power Electronics Section at their university.

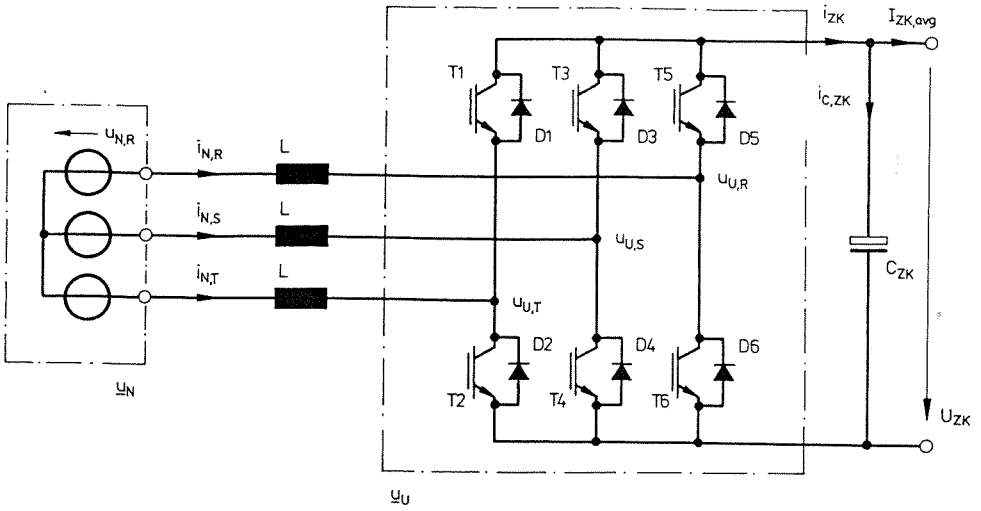

Fig.1: Structure of the power circuit of a three phase voltage DC link PWM converter system. For usage as *PWM inverter* for AC machine drives the inductances L and the three phase system $\underline{u}_N$ can be interpreted as simple equivalent circuit of the AC machine formed by leakage inductances and machine counter emf. On the other hand, for mains operation of the PWM *converter* (PWM rectifier, static VAR compensator) the inductances have to be connected in series; the voltage system $\underline{u}_N$ is defined by the mains conditions.

angle optimization methods (Ref.[6]). Compared to that, in the intermediate and in the lower power regions one aims at high switching frequencies (very high pulse rates) relative to the output frequency. This is made possible especially by the essential progress made in the area of developing of voltage controlled turn-off devices (IGBTs) and in the area of signal electronics. Caused by the computation time rising much more than proportional with the number of switching angles to be determined an application of the classical (conventional) pulse pattern optimization mentioned is hardly possible for high pulse rates.

The calculation of optimal control methods (and, equivalent, of optimal modulation functions for PWM converter systems with high pulse rate) is the object of this paper.

If one can assume approximations which show good consistency with the exact solutions for high system pulse frequencies one can reduce the variational problem of the output current harmonics minimization to a simple extreme value problem. This gives directly the shape of the phase modulation functions of an appropriately optimized modulation method. Contrary to the classical pulse pattern optimization methods thereby the computationally involved optimization of a quality functional by digital computer can be omitted.

The starting point of the optimization is the determination of the parameters of the modulation method which can be treated by an optimization method. There a representation as clear as possible of the existing relationships in the form of a transformation of the system variables into associated space vectors is advantageous.

2 Voltage Generation of a PWM Converter System

The space vector of the output voltage of a PWM converter system (see Fig.1)

$$\underline{u}_U = \frac{2}{3} U_{ZK} \left[u_{U,R} + \underline{a}\, u_{U,S} + \underline{a}^2\, u_{U,T} \right] \qquad \underline{a} = (-\frac{1}{2} + j\frac{\sqrt{3}}{2}) \tag{1}$$

is determined via the switching status. According to Figs.2 and 3 we have:

$$\frac{\delta_6}{\delta_2} = \frac{\sin(\frac{2\pi}{3} - \varphi_U)}{\sin(\varphi_U - \frac{\pi}{3})} \qquad \varphi_U \in \left[\frac{\pi}{3}, \frac{2\pi}{3}\right] \tag{2}$$

$$\underline{u}_U^*(\tau) = \frac{2}{T_P}\left[\int_{t_{\mu,1}(\tau)}^{t_{\mu,2}(\tau)} \underline{u}_{U,6}\, dt_\mu + \int_{t_{\mu,2}(\tau)}^{t_{\mu,3}(\tau)} \underline{u}_{U,2}\, dt_\mu\right] \tag{3}$$

$$\underline{u}_U^* = \hat{\underline{U}}_U^* \exp j\omega_N\tau \tag{4}$$

$$\begin{aligned} \underline{u}_{U,6} &= -\underline{a}^2\,\frac{2}{3}\,U_{ZK} \\ \underline{u}_{U,2} &= +\underline{a}\,\frac{2}{3}\,U_{ZK} \end{aligned} \tag{5}$$

$$\delta_6 = \frac{2}{T_P}\left[t_{\mu,2} - t_{\mu,1}\right] \qquad \delta_2 = \frac{2}{T_P}\left[t_{\mu,3} - t_{\mu,2}\right] \tag{6}$$

$$\underline{u}_U^*(\varphi_U) = \underline{u}_{U,6}\,\delta_6 + \underline{u}_{U,2}\,\delta_2 \qquad \varphi_U = \omega_N\tau \tag{7}$$

$$u_U^*(\varphi_U) = \frac{2}{3}U_{ZK}\left[\delta_6\cos(\varphi_U - \frac{\pi}{3}) + \delta_2\cos(\frac{2\pi}{3} - \varphi_U)\right] \tag{8}$$

$$u_{U,6} = |\underline{u}_{U,6}| = u_{U,2} = |\underline{u}_{U,2}| = \frac{2}{3}U_{ZK} \tag{9}$$

(the indices denote the converter switching state by the decimal equivalent of the converter switching status vector interpreted as binary number). There one basically has to distinguish between the microscopic or local time behavior (t_μ; $t_\mu \in [0, T_P/2]$) of the quantities within a pulse (half) period T_P and the macroscopic (or global) time behavior (τ or angle φ_U – identification of the pulse interval position within the fundamental period) of the quantities which are based on time averaging over a pulse period. For the possible range of the modulation depth

$$M = \frac{2\hat{U}_{U,(1)}}{U_{ZK}} = \frac{2\hat{U}_U^*}{U_{ZK}} \tag{10}$$

there follows (see Fig.2)

$$M \in \left[0, \frac{2}{\sqrt{3}}\right] \;; \qquad |\hat{U}_U^*| \in \left[0, \frac{U_{ZK}}{\sqrt{3}}\right] . \tag{11}$$

The equations (2) and (8) are valid independently of the modulation method selected. The equations define the shape of the phase modulation functions $m_{(RST)}(\tau)$ (or $\alpha_{(RST)}$, respectively) via

$$\begin{aligned} \delta_6 &= (\alpha_R - \alpha_T) \\ \delta_2 &= (\alpha_S - \alpha_R) \end{aligned} \tag{12}$$

$$\delta_0 + \delta_7 = 1 - (\alpha_S - \alpha_T)$$

$$\begin{aligned} \delta_7 &= \alpha_T \\ \delta_0 &= (1 - \alpha_S) \end{aligned} \tag{13}$$

with

$$\begin{aligned} \alpha_R(\tau) &= \frac{2t_{\mu,2}}{T_P} = \frac{1}{2}\left[1 + m_R(\tau)\right] \\ \alpha_S(\tau) &= \frac{2t_{\mu,3}}{T_P} = \frac{1}{2}\left[1 + m_S(\tau)\right] \\ \alpha_T(\tau) &= \frac{2t_{\mu,1}}{T_P} = \frac{1}{2}\left[1 + m_T(\tau)\right] . \end{aligned} \tag{14}$$

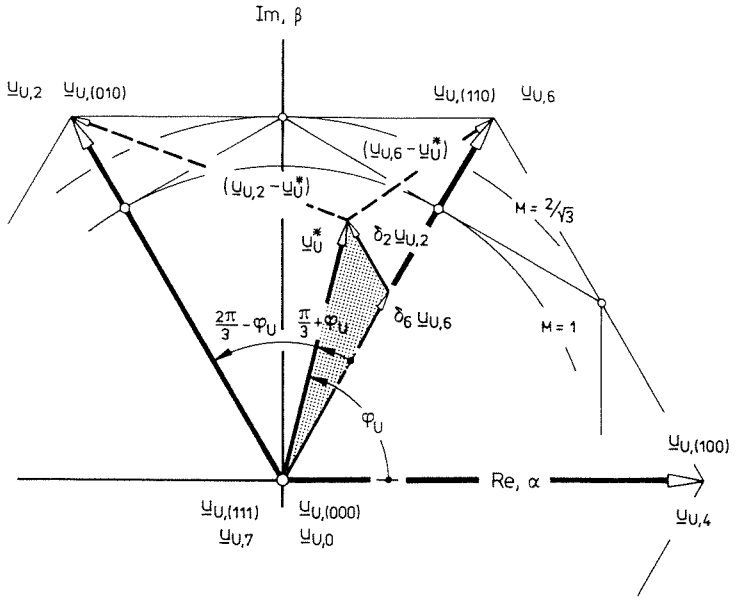

Fig.2: Approximation of the reference value of the converter output voltage via neighbouring converter voltage space vectors (due to the 60^o–symmetry of the voltage space vectors following for the remaining converter switching states one can limit the considerations to the interval of φ_U shown here).

As parameter which can be freely choosen there remains the distribution of the non-voltage-forming free-wheeling status $(\delta_0 + \delta_7)$ between begin and end of each half pulse period. Via an optimizing calculation one can therefore select one modulation function (which gives the extreme for a given optimization criterion) among the infinitely large number of possible modulation functions.

Note: The equations (2) and (8) naturally are fulfilled also for a sinusoidal shape of the modulation functions

$$\begin{aligned} \alpha_R &= \frac{1}{2} + \frac{M}{2} \cos \omega_N \tau \\ \alpha_S &= \frac{1}{2} + \frac{M}{2} \cos \left(\omega_N \tau - \frac{2\pi}{3} \right) \\ \alpha_T &= \frac{1}{2} + \frac{M}{2} \cos \left(\omega_N \tau + \frac{2\pi}{3} \right) \end{aligned} \tag{15}$$

(subharmonic modulation method). This, however, determines directly the distribution of the free-wheeling status

$$\delta_7 + \delta_0 = 1 - \frac{\sqrt{3} M}{2} \sin \varphi_U \tag{16}$$

where

$$\begin{aligned} \delta_7 &= \frac{1}{2} + \frac{M}{2} \cos \left(\varphi_U + \frac{\pi}{3} \right) \\ \delta_0 &= \frac{1}{2} - \frac{M}{2} \cos \left(\varphi_U - \frac{\pi}{3} \right) . \end{aligned} \tag{17}$$

Furthermore, the limit towards overmodulation is given by

$$M \in [0, 1] . \tag{18}$$

Each function $m_0(\tau)$ with a general shape (e.g., third harmonic) which is added to the simplest (purely sinusoidal) modulation functions $m'_{(RST)}$

$$\begin{aligned} m_R &= m'_R + m_0 \\ m_S &= m'_S + m_0 \end{aligned}$$

$$m_T = m'_T + m_0 \qquad (19)$$
$$m_0 = \frac{1}{3}(m_R + m_S + m_T)$$

$$m_{(RST)}(\tau) = \frac{2}{U_{ZK}}\, u_{U,(RST)}(\tau) = 2\alpha_{(RST)}(\tau) - 1 \qquad m_{(RST)} \in [-1, +1] \qquad (20)$$

influences only the distribution of the non-voltage-forming status. Being a zero quantity, $m_0(\tau)$ is not projected into the space vector of the converter voltage or into the line-to-line voltage.

3 Optimization for Continuous Modulation

In the following such modulation functions are defined as being continuous which show a continuous time behavior of the associated phase modulation functions. This means that according to a switching state sequence

$$\ldots 0\ 2\ 6\ 7\Big|_{t_\mu=0}\ 7\ 6\ 2\ 0\Big|_{t_\mu=T_P/2}\ 0\ 2\ 6\ 7\ldots \qquad \varphi_U \in \left[\frac{\pi}{3}, \frac{2\pi}{3}\right] \qquad (21)$$

within a fundamental period always all bridge legs of the converter system are switched with pulse frequency. The generation of phase voltages which have a sinusoidal form in the time average over a pulse period is common to all these modulation methods. A deviation from the sinusoidal shape can be given according to a zero quantity $m_0(\tau)$. This modulation function portion which has to be set during the optimization calculus in any case shows time continuous behavior for continuous modulation. As reference point for the phase voltages the ficticious center point of the DC link voltage is chosen. The line to line voltages of the three wire system have to be calculated from the phase voltages via forming the differences (there the zero sequence system is decoupled). As shown in the following now one can choose as reference potential of the phase generated voltage system not only the DC link voltage center point but alternating the positive and negative DC link voltage bus. This is equivalent to setting the switching status of always one converter bridge leg within an interval of a fundamental period where this setting changes cyclically between the phases. The two remaining converter phases can be controlled via pulse width modulation in such a way that the (line to line) voltages related to the third "clamped" phase again show a sinusoidal form in their time average for a pulse period. These modulation methods which represent a specific case of the continuous modulation are called discontinuous modulation in the following due to the discontinuous behavior of the associated modulation functions (or, of the associated zero quantity m_0, respectively). They are analyzed in chapter 4 in more detail.

For continuous modulation as quality functional

$$I = \Delta I^2_{N,RST,rms} = \frac{1}{T_N}\int_{T_N} \Delta i^2_{N,RST,rms}(\tau)\, d\tau \rightarrow Min \qquad (22)$$

we will select the integral (related to the fundamental period) of the square of the deviation

$$\Delta \underline{i}_N = \underline{i}_N - \underline{i}^*_N \qquad (23)$$

between the current actual and reference value

$$\underline{i}^*_N(\tau) = \hat{\underline{I}}^*_N \exp j\omega_N \tau \qquad (24)$$

shapes or the rms value of the current harmonics. For its calculation one can choose a simple equivalent circuit of the fed system (considering the high pulse rate assumed) according to

$$L\,\frac{d\underline{i}_N}{dt} = (\underline{u}_U - \underline{u}_N)\ . \qquad (25)$$

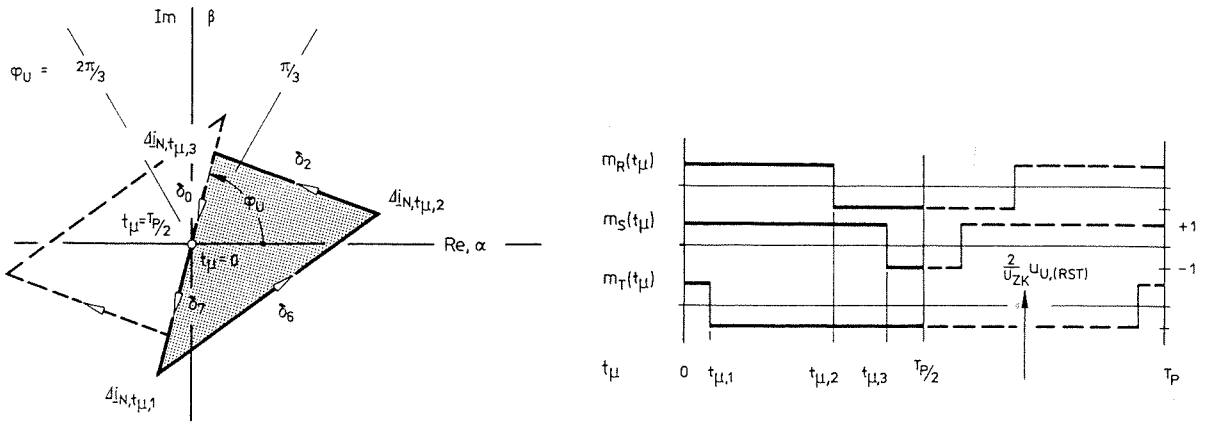

Fig.3: left: Trajectory of the space vector $\Delta\underline{i}_N(t_\mu)$ within one pulse half period; right: associated microscopic time behavior of the phase modulation functions (pulse pattern).

For the space vector of $\Delta\underline{i}_N$ there follows (see Fig.3)

$$\frac{d\Delta\underline{i}_N}{dt_\mu} = \frac{1}{L}\left[\underline{u}_U - \underline{u}_U^*(\tau)\right] \tag{26}$$

$$\begin{aligned}
\Delta\underline{i}_{N,t_{\mu,1}}(\tau) &= \delta_7\left[-\underline{u}_U^*(\tau)\right]\frac{T_P}{2L} \\
\Delta\underline{i}_{N,t_{\mu,2}}(\tau) &= \Delta\underline{i}_{N,t_{\mu,1}}(\tau) + \delta_6\left[\underline{u}_{U,6} - \underline{u}_U^*(\tau)\right]\frac{T_P}{2L} \\
\Delta\underline{i}_{N,t_{\mu,3}}(\tau) &= \Delta\underline{i}_{N,t_{\mu,2}}(\tau) + \delta_2\left[\underline{u}_{U,2} - \underline{u}_U^*(\tau)\right]\frac{T_P}{2L}
\end{aligned} \tag{27}$$

or

$$\begin{aligned}
\Delta\underline{i}_{N,t_{\mu,2}}(\tau) &= \delta_6\underline{u}_{U,6}\frac{T_P}{2L} - (\delta_7+\delta_6)\,\underline{u}_U^*(\tau)\frac{T_P}{2L} \\
\Delta\underline{i}_{N,t_{\mu,3}}(\tau) &= \delta_0\underline{u}_U^*(\tau)\frac{T_P}{2L}\,,
\end{aligned} \tag{28}$$

respectively, with

$$L\,\frac{d\underline{i}_N^*}{dt} = (\underline{u}_U^* - \underline{u}_N) \tag{29}$$

and

$$\begin{aligned}
\underline{u}_U^*(\tau) &= \underline{u}_N(\tau) + j\omega L\,\underline{i}_N^*(\tau) \\
\underline{i}_N^*(\tau+t_\mu) &= \underline{i}_N^*(\tau) + j\omega t_\mu\,\underline{i}_N^*(\tau)
\end{aligned} \tag{30}$$

(approximation of the circular trajectory of the reference-current space vector by the local tangent). Then we have

$$\Delta\underline{i}_{N,\frac{1}{2}T_P}(\tau) = \underline{i}_{N,t_{\mu,3}}(\tau) - \delta_0\underline{u}_U^*(\tau)\,\frac{T_P}{2L} = 0 \tag{31}$$

with

$$\underline{u}_U^*(\tau) = \delta_6(\tau)\,\underline{u}_{U,6} + \delta_2(\tau)\,\underline{u}_{U,2} \tag{32}$$

or

$$\underline{i}_N^*(\tau + \frac{T_P}{2}) = \left(1 + j\omega_N \frac{T_P}{2}\right) \underline{i}_N^*(\tau) \ , \tag{33}$$

respectively. As is shown by a simple consideration, one can formulate the sum of the squares of the phase currents via the α,β-coordinates of the related space vector

$$\Delta i_{N,R}^2 + \Delta i_{N,S}^2 + \Delta i_{N,T}^2 = \frac{3}{2}[\Delta i_{N,\alpha}^2 + \Delta i_{N,\beta}^2] = \frac{3}{2}|\Delta \underline{i}_N|^2 \ . \tag{34}$$

With this, Eq.(27) and

$$\frac{1}{(t_{\mu,i+1} - t_{\mu,i})} \int_{t_{\mu,i}}^{t_{\mu,i+1}} \left[\Delta i_{N,\alpha}^2(t_\mu) + \Delta i_{N,\beta}^2(t_\mu)\right] dt_\mu = \tag{35}$$

$$\frac{1}{3}\left[\left(\Delta i_{N,i,\alpha}^2 + \Delta i_{N,i,\alpha}\Delta i_{N,i+1,\alpha} + \Delta i_{N,i+1,\alpha}^2\right) + \left(\Delta i_{N,i,\beta}^2 + \Delta i_{N,i,\beta}\Delta i_{N,i+1,\beta} + \Delta i_{N,i+1,\beta}^2\right)\right] \tag{36}$$

the local rms value (related to a pulse (half) interval) of the current ripple can be expressed according to

$$\Delta i_{N,RST,rms}^2(\tau) = \frac{2}{T_P} \int_{t_\mu=0}^{t_\mu=\frac{1}{2}T_P} \left[\Delta i_{N,R}^2(t_\mu) + \Delta i_{N,S}^2(t_\mu) + \Delta i_{N,T}^2(t_\mu)\right] \ dt_\mu =$$

$$\begin{aligned}
\tfrac{1}{2}\Big\{\delta_7 \quad & \left[\Delta i_{N,t_{\mu,1},\alpha}^2 + \Delta i_{N,t_{\mu,1},\beta}^2\right] \\
+\delta_6 \quad & \left[\Delta i_{N,t_{\mu,1},\alpha}^2 + \Delta i_{N,t_{\mu,1},\beta}^2 + \Delta i_{N,t_{\mu,2},\alpha}^2 + \Delta i_{N,t_{\mu,2},\beta}^2 + \Delta i_{N,t_{\mu,1},\alpha}\Delta i_{N,t_{\mu,2},\alpha} + \Delta i_{N,t_{\mu,1},\beta}\Delta i_{N,t_{\mu,2},\beta}\right] \\
+\delta_2 \quad & \left[\Delta i_{N,t_{\mu,2},\alpha}^2 + \Delta i_{N,t_{\mu,2},\beta}^2 + \Delta i_{N,t_{\mu,3},\alpha}^2 + \Delta i_{N,t_{\mu,3},\beta}^2 + \Delta i_{N,t_{\mu,2},\alpha}\Delta i_{N,t_{\mu,3},\alpha} + \Delta i_{N,t_{\mu,2},\beta}\Delta i_{N,t_{\mu,3},\beta}\right] \\
+\delta_0 \quad & \left[\Delta i_{N,t_{\mu,3},\alpha}^2 + \Delta i_{N,t_{\mu,3},\beta}^2\right]\Big\}
\end{aligned} \tag{37}$$

with

$$\delta_0 = 1 - (\delta_7 + \delta_6 + \delta_2) \ . \tag{38}$$

For the calculation of the global rms value (being set equal to the quality functional I) related to the fundamental period we have

$$\begin{aligned}
I = \Delta I_{N,RST,rms}^2 &= \frac{1}{T_N} \int_{T_N} (\Delta i_{N,R}^2 + \Delta i_{N,S}^2 + \Delta i_{N,T}^2)\, dt \\
&= \frac{1}{T_N} \sum_j \int_{\frac{1}{2}T_P(j)} (\Delta i_{N,R}^2 + \Delta i_{N,S}^2 + \Delta i_{N,T}^2)\, dt_\mu \ .
\end{aligned} \tag{39}$$

Now, in the sense of a simple averaging of the local harmonic loss contributions the position of the pulse interval shall be moved time-continuously through the fundamental period. Then with sufficiently good approximation for high pulse frequency, the summation due to the finite system switching frequency can be replaced by an integration. This allows to calculate a simple analytical expression for the harmonic power loss

$$\begin{aligned}
I = \Delta I_{N,RST,rms}^2 &= \frac{1}{T_N} \int_{T_N} \{\frac{2}{T_P} \int_{t_\mu=0}^{t_\mu=\frac{1}{2}T_P} (\Delta i_{N,R}^2 + \Delta i_{N,S}^2 + \Delta i_{N,T}^2)\, dt_\mu\}\, d\tau \\
&= \frac{1}{T_N} \int_{T_N} \Delta i_{N,RST,rms}^2(\tau)\, d\tau \rightarrow Min \ .
\end{aligned} \tag{40}$$

A minimization of the quality functional therefore is given via the minimization of the local (always positive) contribution

$$\Delta i_{N,RST,rms}^2(\tau) \rightarrow Min \ , \tag{41}$$

i.e. the local harmonic rms value

$$\Delta i^2_{N,RST,rms}(\tau) = \Delta i^2_{N,RST,rms,1}\{\delta_7(\tau),\delta_6(\tau),\delta_2(\tau)\} + \Delta i^2_{N,RST,rms,2}\{\delta_6(\tau),\delta_2(\tau)\} \tag{42}$$

$$\begin{aligned}
\frac{1}{\Delta i_n^2}\Delta i^2_{N,RST,rms,1} &= \frac{48}{9}\delta_7\Big\{\delta_2\delta_6(\delta_2-\delta_6) - 2\delta_{26}\left[1-(\delta_7+\delta_6+\delta_2)\right]\Big\} \\
\frac{1}{\Delta i_n^2}\Delta i^2_{N,RST,rms,2} &= \frac{16}{9}\Big\{6\delta_{26}^2 + 2\delta_{26} - 4\delta_2^4 - 4\delta_6^4 - 4\delta_2\delta_{26} - 4\delta_6\delta_{26} - \\
&- 8\delta_2\delta_6\delta_{26} + 2\delta_2\delta_6^2 - \delta_2^2\delta_6 + 3\delta_2^3\delta_6 - \delta_2^2\delta_6^2\Big\}
\end{aligned} \tag{43}$$

with

$$\Delta i_n^2 = \frac{U_{ZK}T_P}{8L} \tag{44}$$

and

$$\delta_{26} = \delta_2^2 + \delta_2\delta_6 + \delta_6^2 \; . \tag{45}$$

The variational problem at hand (minimization of the quality functional I via determination of the optimal time behavior of $\delta_7(\tau)$) thereby can be reduced to a simple extreme value problem.

Then the optimal distribution of the free-wheeling state has to be set according to

$$\frac{d}{d\delta_7}\{\Delta i^2_{N,RST,rms}\}\big|_{\tau=const} = 0 \tag{46}$$

in connection with

$$\delta_{7,I=Min} = \{\frac{1}{2}[1-(\delta_2+\delta_6)] - \frac{\delta_2\delta_6}{4\delta_{26}}(\delta_2-\delta_6)\} \; . \tag{47}$$

With this, as a simple and clear suboptimal approximation we receive

$$\delta_{7,[2]} = \frac{1}{2}[1-(\delta_2+\delta_6)] = \frac{1}{2}(\delta_0+\delta_7) = \frac{1}{2} - \frac{\sqrt{3}M}{4}\sin\varphi_U \; . \tag{48}$$

For the global harmonic current rms value there follows

$$\boxed{\Delta I^2_{N,rms,[2]} = \frac{1}{6}\Delta i_n^2 M^2\left[1 - \frac{8M}{\sqrt{3}\pi} + \frac{9M^2}{8}\left(1-\frac{3\sqrt{3}}{4\pi}\right)\right]} \qquad M \in \left[0, \frac{2}{\sqrt{3}}\right] \; . \tag{49}$$

If we compare this with the evaluation of Eq.(40) for simple sinusoidal modulation

$$\delta_{7,[1]} = \frac{1}{2} + \frac{M}{2}\cos(\varphi_U + \frac{2\pi}{3}) \tag{50}$$

$$\boxed{\Delta I^2_{N,rms,[1]} = \frac{1}{6}\Delta i_n^2 M^2\left[1 - \frac{8M}{\sqrt{3}\pi} + \frac{3M^2}{4}\right]} \tag{51}$$

for which the distribution of the non-voltage forming state is given by Eq.(17) one can see (according to Fig.9) a substantial reduction of the harmonic losses, especially in the upper modulation region. An illustration of the modulation method can be given via the representation of the phase modulation functions

$$\begin{aligned}
[2]: \; M \le \frac{2}{\sqrt{3}};\;\; \varphi_U \in \left[\frac{\pi}{3}, \frac{2\pi}{3}\right]: \qquad m_R &= \frac{3}{2}M\cos\varphi_U \\
m_S &= \frac{\sqrt{3}M}{2}\sin\varphi_U \\
m_T &= -\frac{\sqrt{3}M}{2}\sin\varphi_U \\
m_0 &= \frac{M}{2}\cos\varphi_U
\end{aligned} \tag{52}$$

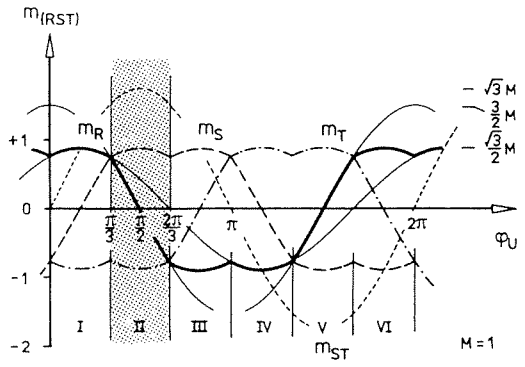

Fig.4: Shape of the phase modulation function according to Eq.(52) or [2], respectively

(cf. Fig.4 or Refs.[1],[3], respectively).

4 Optimization for Discontinuous Modulation

The basic idea behind the optimization calculation outlined above is the determination of the distribution of the non-voltage-forming states between begin and end of each pulse half period according to a switching status sequence

$$\ldots 0\ 2\ 6\ 7\Big|_{t_\mu=0}\ 7\ 6\ 2\ 0\Big|_{t_\mu=T_P/2}\ 0\ 2\ 6\ 7\ldots \tag{53}$$

If now the entire free-wheeling state of a pulse period is concentrated at its begin (or end)

$$\begin{aligned} \delta_7 &= 1-(\delta_2+\delta_6) \\ \delta_0 &= 0 \end{aligned} \tag{54}$$

$$\ldots 2\ 6\ 7\Big|_{t_\mu=0}\ 7\ 6\ 2\Big|_{t_\mu=T_P/2}\ 2\ 6\ 7\ldots \tag{55}$$

$$\Delta i^2_{N,RST,rms}(\tau) = \Delta i^2_{N,RST,rms,1}(\tau) + \Delta i^2_{N,RST,rms,2}(\tau) \tag{56}$$

or

$$\begin{aligned} \delta_7 &= 0 \\ \delta_0 &= 1-(\delta_2+\delta_6) \end{aligned} \tag{57}$$

$$\ldots 0\ 2\ 6\Big|_{t_\mu=0}\ 6\ 2\ 0\Big|_{t_\mu=T_P/2}\ 0\ 2\ 6\ldots \tag{58}$$

$$\Delta i^2_{N,RST,rms}(\tau) = \Delta i^2_{N,RST,rms,2}(\tau) \tag{59}$$

in any case an increase of the harmonic losses is to be expected relative to the optimized result. A closer analysis of the resulting switching state sequence shows, however, that then (under observation of the three-phase property) one bridge leg is not being pulsed within one third of the fundamental period (denoted as discontinuous modulation, see section 3). For equal global switching losses thereby the switching frequency for this control method can be selected higher by the factor (see Fig.5 or Ref.[4], respectively)

$$\begin{aligned} k_{f,[4]} = \frac{f_{P,[4]}}{f_P} &= \frac{1}{\left[1-\frac{(\sqrt{3}-1)}{2}\cos\varphi\right]} && \varphi\in[0,\tfrac{\pi}{6}] \\ &= \frac{2}{[\sin\varphi+\cos\varphi]} && \varphi\in[\tfrac{\pi}{6},\tfrac{\pi}{3}] \\ &= \frac{1}{\left[1-\frac{(\sqrt{3}-1)}{2}\sin\varphi\right]} && \varphi\in[\tfrac{\pi}{3},\tfrac{\pi}{2}] \end{aligned} \tag{60}$$

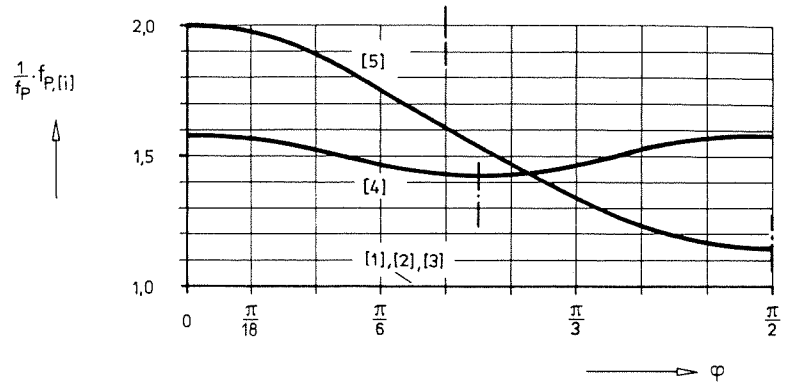

Fig.5: Possible frequency increase $k_{f,i}$ of the modulation methods [4], [5] in comparison to "continuous" modulation methods [1], [2], [3] (e.g., simple sinusoidal modulation).

or

$$k_{f,[5]} = \frac{f_{P,[5]}}{f_P} = \begin{cases} \dfrac{1}{\left(1 - \frac{1}{2}\cos\varphi\right)} & \varphi \in [0, \frac{\pi}{3}] \\ \dfrac{2}{\sqrt{3}\sin\varphi} & \varphi \in [\frac{\pi}{3}, \frac{\pi}{2}] \end{cases} \tag{61}$$

(There the modulation method is defined in dependency of the angle φ between the fundamental of the converter output voltage and the phase current). This leads to a corresponding shift of the audible noise producing frequencies to higher frequencies. There a dependency

$$w_{P,(TD)}\{i_T(\omega_N\tau)\} = k_{1,(TD)}\, i_{(TD)}(\omega_N\tau) \tag{62}$$

$$p_{P,(TD)} = w_{P,(TD)} f_P \tag{63}$$

between the sum of turn-on and turn-off losses $p_{P,(TD)}$ and the switched current is assumed, a dependency which approximates the actual relationships sufficiently accurately and which is described by the factor $k_{1,(TD)}$. Averaging of this switching loss (related to a position of a pulse interval) for a positive (or negative) output current half period leads for "continous" modulation (e.g., sinusoidal modulation or [1] in Fig.5, respectively) to a global switching loss of a transistor-diode-pair of a bridge leg (e.g., T_2 and D_1 in Fig.1)

$$P_{P,T1,D2} = \hat{I}_N f_P \frac{k_{1,T,D}}{\pi} \tag{64}$$

with

$$k_{1,T,D} = k_{1,T} + k_{1,D}\ . \tag{65}$$

As a calculation of the local harmonic current rms values

$$\Delta i^2_{N,RST,rms,1}(\varphi_U)\Big|_{\delta_7 = 1-(\delta_2+\delta_6)} = \begin{cases} \leq 0 & \varphi_U \in \left[\frac{\pi}{3}, \frac{\pi}{2}\right] \\ \geq 0 & \varphi_U \in \left[\frac{\pi}{2}, \frac{2\pi}{3}\right] \end{cases} \tag{66}$$

shows a minimization of the global harmonic losses is given for a cyclic change

$$\delta_{7,[4]} = \begin{cases} 1 - (\delta_2 + \delta_6) & \varphi_U \in \left[\frac{\pi}{3}, \frac{\pi}{2}\right] \\ 0 & \varphi_U \in \left[\frac{\pi}{2}, \frac{2\pi}{3}\right] \end{cases} \tag{67}$$

$$\delta_{7,[5]} = \begin{cases} 0 & \varphi_U \in \left[\frac{\pi}{3}, \frac{\pi}{2}\right] \\ 1 - (\delta_2 + \delta_6) & \varphi_U \in \left[\frac{\pi}{2}, \frac{2\pi}{3}\right] \end{cases}, \tag{68}$$

between the two possible, simplified switching state sequences. A more detailed discussion has to be omitted here for the sake of brevity.

For the global harmonic losses there results

$$\boxed{\Delta I^2_{N,rms,[4]} = \frac{1}{6}\Delta i_n^2 M^2 \frac{1}{k^2_{f,[4]}}\left[4 - \frac{M}{\sqrt{3}\pi}\left(62 - 15\sqrt{3}\right) + \frac{9M^2}{8}\left(2 + \frac{\sqrt{3}}{\pi}\right)\right]} \tag{69}$$

or

$$\boxed{\Delta I^2_{N,rms,[5]} = \frac{1}{6}\Delta i_n^2 M^2 \frac{1}{k^2_{f,[5]}}\left[4 - \frac{M}{\sqrt{3}\pi}\left(8 + 15\sqrt{3}\right) + \frac{9M^2}{8}\left(2 + \frac{\sqrt{3}}{2\pi}\right)\right]} \tag{70}$$

respectively with

$$k_{f,[n]} = \frac{f_{P,[n]}}{f_P} \tag{71}$$

(cf. Fig.9).

Equation (70) defines quantitatively a variant of the optimal control method. The modulation functions related to Eqs.(69) and (70)

$$\begin{aligned}
[4]:\ M \le \frac{2}{\sqrt{3}} \qquad \varphi_U \in \left[\frac{\pi}{3}, \frac{\pi}{2}\right]: \quad m_R &= 1 - \sqrt{3}M\sin\left(\varphi_U - \frac{\pi}{3}\right) \\
m_S &= +1 \\
m_T &= 1 - \sqrt{3}M\sin\varphi_U \\
m_0 &= 1 + M\cos\left(\varphi_U + \frac{\pi}{3}\right) \\
\varphi_U \in \left[\frac{\pi}{2}, \frac{2\pi}{3}\right]: \quad m_R &= \sqrt{3}M\sin\left(\varphi_U + \frac{\pi}{3}\right) - 1 \\
m_S &= \sqrt{3}M\sin\varphi_U - 1 \\
m_T &= -1 \\
m_0 &= M\sin\left(\varphi_U + \frac{\pi}{6}\right) - 1
\end{aligned} \tag{72}$$

and

$$\begin{aligned}
[5]:\ M \le \frac{2}{\sqrt{3}} \qquad \varphi_U \in \left[\frac{\pi}{3}, \frac{\pi}{2}\right]: \quad m_R &= \sqrt{3}M\sin\left(\varphi_U + \frac{\pi}{3}\right) - 1 \\
m_S &= \sqrt{3}M\sin\varphi_U - 1 \\
m_T &= -1 \\
m_0 &= M\sin\left(\varphi_U + \frac{\pi}{6}\right) - 1 \\
\varphi_U \in \left[\frac{\pi}{2}, \frac{2\pi}{3}\right]: \quad m_R &= 1 - \sqrt{3}M\sin\left(\varphi_U - \frac{\pi}{3}\right) \\
m_S &= +1 \\
m_T &= 1 - \sqrt{3}M\sin\varphi_U \\
m_0 &= 1 + M\cos\left(\varphi_U + \frac{\pi}{3}\right)
\end{aligned} \tag{73}$$

respectively, are shown in Figs.6,7.

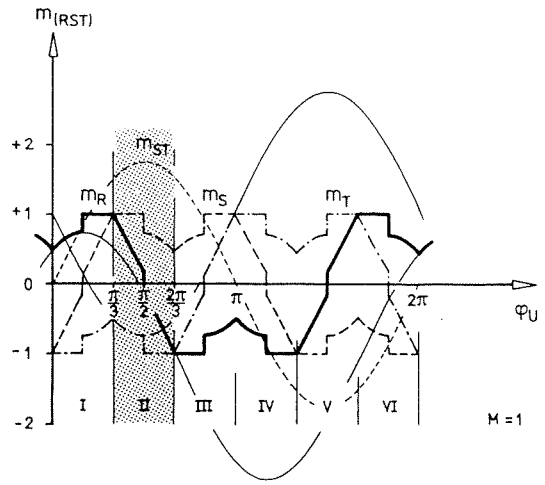

Fig.6: Shape of the phase modulation function according to Eq.(72) or [4], respectively

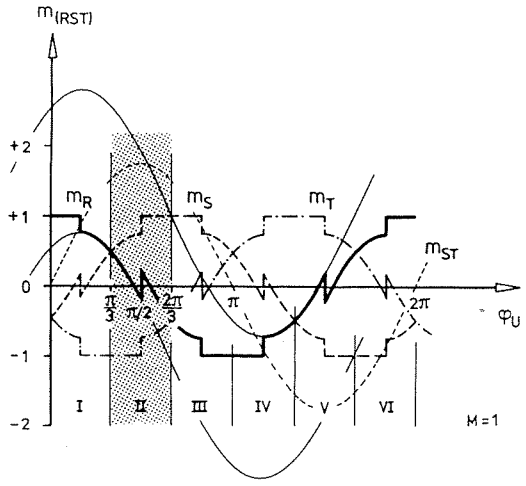

Fig.7: Shape of the phase modulation function according to Eq.(73) or [5], respectively

5 Direct Optimization via Phase Modulation Functions

In conclusion we want to briefly treat the direct optimization of a modulation function without the detour of analyzing the local harmonic power loss contributions. With given shape of one phase modulation function triple the pulse pattern is completly determined (cf. Eqs.(14)) and therefore also the local distribution of the free-wheeling state Eq.(13). Effecting this is only possible in a global way via the time behavior of a parameter determing the modulation functions, such as the amplitude of a third harmonic being added to the simple phase modulation functions of purely sinusoidal shape

$$\begin{aligned} m_R(\varphi_U) &= M_1 \cos\varphi_U - \frac{M_3}{2}\cos 3\varphi_U \\ m_S(\varphi_U) &= M_1 \cos\left(\varphi_U - \frac{2\pi}{3}\right) - \frac{M_3}{2}\cos 3\varphi_U \\ m_T(\varphi_U) &= M_1 \cos\left(\varphi_U + \frac{2\pi}{3}\right) - \frac{M_3}{2}\cos 3\varphi_U \end{aligned} \tag{74}$$

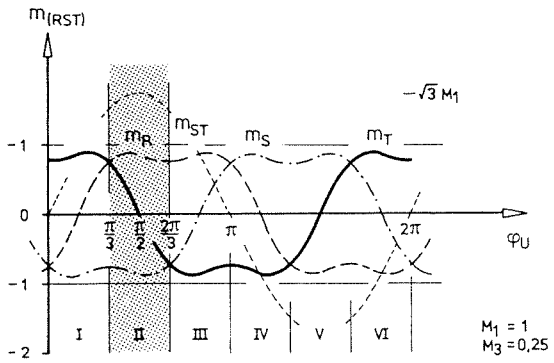

Fig.8: Shape of the phase modulation function according to Eqs.(74),(78) or [3], respectively

or

$$m_0 = -\frac{M_3}{2}\cos 3\varphi_U \ . \tag{75}$$

For the global rms value of the harmonic power losses there follows then a functional dependency of the global harmonic losses according to

$$\Delta I^2_{N,rms} = \Delta I^2_{N,rms}\left\{M_3^2 - M_3\frac{M_1}{2}\right\} \tag{76}$$

with

$$M_3 = \frac{2\hat{U}^*_{U,(3)}}{U_{ZK}} \ . \tag{77}$$

The determination of the optimal relationship minimizing the harmonic power loss

$$\left.\frac{M_3}{M_1}\right|_{I=min} = \frac{1}{4} \tag{78}$$

therefore can simply be achieved again in the form of solving an extreme value problem (cf. Fig.8 and Fig.9, respectively). **It is of basic importance to state that therefore the global and local (see section 3, Eq.47) optimization according to**

$$\delta_{7,I=Min} = \{\frac{1}{2}[1-(\delta_2+\delta_6)] - \frac{\delta_2\delta_6}{4\delta_{26}}(\delta_2-\delta_6)\} = \delta_{7,[3]} = \frac{1}{2}[1+m_T(\varphi_U)] \tag{79}$$

with

$$m_T(\varphi_U) = \frac{1}{2} + \frac{M_1}{2}\cos\left(\varphi_U + \frac{2\pi}{3}\right) - \frac{M_1}{8}\cos 3\varphi_U \tag{80}$$

lead to identical minima !! The modulation limit there is given by

$$\left.M_{1,max}\right|_{\frac{M_3}{M_1}=\frac{1}{4}} = 0.972\ \frac{2}{\sqrt{3}} \ , \tag{81}$$

however. The harmonic power loss rms value thereby can be calculated as

$$\boxed{\Delta I^2_{N,rms,[3]} = \frac{1}{6}\Delta i_n^2 M_1^2\left\{1 - \frac{8M_1}{\sqrt{3}\pi} + \frac{3M_1^2}{4}\left[1 - \frac{M_3}{M_1}\left(1 - 2\frac{M_3}{M_1}\right)\right]\right\}} \ . \tag{82}$$

For an optimization of the maximum possible modulation there follows

$$\left.\frac{M_3}{M_1}\right|_{I\approx min} = \frac{1}{6} \qquad M \in \left[0, \frac{2}{\sqrt{3}}\right] \ . \tag{83}$$

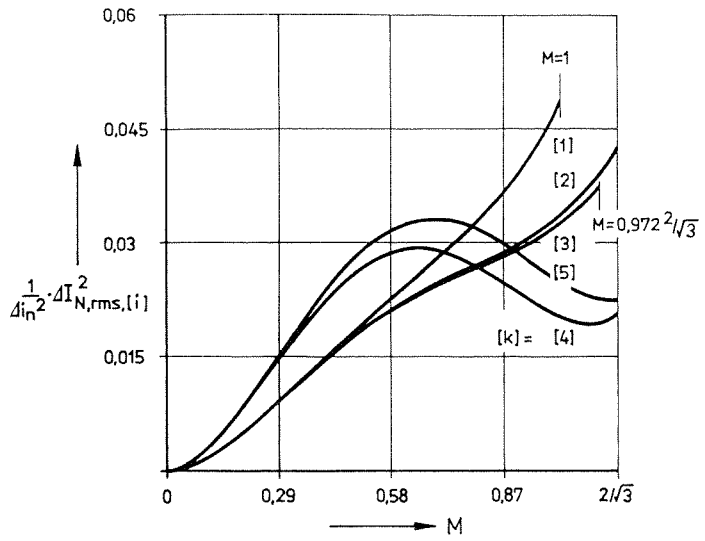

Fig.9: Comparison of the normalized harmonic power losses for various modulation methods ([1]: Sinusoidal modulation (Eq.(51)); [2]: Suboptimal space vector modulation (Eq.(49)); [3]: Local and global optimal sinusoidal modulation with added third harmonic ($M_3 = M_1/4$, verified in sections 3 or 5, respectively; Eq.(82)); [4],[5]: Optimal control methods derived in this paper ($k_{f,[4]} = k_{f,[5]} = 3/2$; Eqs.(69),(70))

6 Comparison of the Optimization Methods and Results

A comparison of all control methods discussed in this paper is shown in Fig.9. A control method based on the simplification of the switching state sequence appears to be especially interesting in connection with PWM rectifier systems because they operate in the stationary case with modulation indexes and $\cos\varphi$ close to one.

A treatment of transferring the control method derived here for voltage DC link PWM converters to current DC link PWM converters has to be omitted here due to space considerations. A detailed representation of this problem area can be found in Ref.[5].

A comparison of the evaluation of the expressions gained with the purely analytical approach with the results of the analysis of the different control methods gained by digital simulation shows very good consistency already for relatively low pulse rates ($pz = 2\pi f_P/\omega_N \geq 21$).

7 Conclusion

The calculation method presented here is based on the application of the space vector calculus and on the introduction of a simple averaging method which approximates the time-discontinuous system motions by time-continuous representation. This calculation method therefore can be used for the optimization of pulse patterns of medium and high pulse rates and also for the determination of the harmonic power loss as used for dimensioning purposes.

From an engineering point of view furthermore especially the presence of an approximate solution as a simple mathematical expression and the broad applicability of the principle presented here for the analysis of power electronic circuits has to be pointed out.

References

[1] **van der Broeck, H. W., Skudelny, H. C., and Stanke, G. V.:** *Analysis and Realization of a Pulsewidth Modulator Based on Voltage Space Vectors.* IEEE Transactions on Industry Application, Vol. IA-24, No.1, 142–150 (1988).

[2] **Ogasawara, S., Akagi, H., and Nabae, A.:** *A Novel PWM Scheme of Voltage Source Inverters based on Space Vector Theory.* Proceedings of the 3rd European Conference on Power Electronics and Applications, Aachen, Oct. 9–12, Vol. 3, 1197–1202 (1989).

[3] **Kolar, J. W., Ertl, H., and Zach, F. C.:** *Calculation of the Passive and Active Component Stress of Three-Phase PWM Converter Systems with High Pulse Rate.* Proceedings of the 3rd European Conference on Power Electronics and Applications, Aachen, Oct. 9–12, Vol. 3, 1303–1311 (1989).

[4] **Kolar, J. W., Ertl, H., and Zach, F. C.:** *Influence of the Modulation Method on the Conduction and Switching Losses of a PWM Converter System.* Proposed for publication on the 25th IAS Annual Meeting, Seattle, Oct. 7–12, (1990).

[5] **Kolar, J. W., Ertl, H., and Zach, F. C.:** *Analysis and Duality of Three-Phase Converters with DC Voltage Link and DC Current Link.* Proceedings of the 24th IAS Annual Meeting, San Diego, Oct. 1–5, Vol. 1, 724–737 (1989).

[6] **Zach, F. C., and Ertl, H.:** *Efficiency Optimal Control for AC Drives with PWM Inverters.* IEEE Transactions on IA, Vol. IA-21, No. 4, 987–1000 (1985).